Deficiency of Rho Kinase 1 (ROCK1) attenuates neutrophil NETosis and ameliorates UVB-induced skin inflammation

Minghui Li[1,2,3†], Xing Lyu[1,2,3†], James Liao[4], Victoria P. Werth[1,2], Ming-Lin Liu[1,2]

[1] Corporal Michael J. Crescenz VAMC, Philadelphia, PA, 19104, USA

[2] Department of Dermatology, Perelman School of Medicine, University of Pennsylvania, Philadelphia, PA, 19104, USA

[3] Department of Rheumatology and Immunology, Tianjin Medical University General Hospital, Tianjin 300052, China

[4] Division of Cardiology, Department of Medicine, University of Chicago, Chicago, IL, USA

[†] Contribution equally

Running title: ***Rho kinase and NETosis***

Key words: ***Rho kinase, Neutrophil, NETosis, UVB, Skin inflammation.***

Correspondence to Ming-Lin Liu, MBBS, PhD, Department of Dermatology, Perelman School of Medicine, University of Pennsylvania, and Philadelphia Veterans Administration Medical center, Philadelphia, PA 19104, eMAIL: lium1@pennmedicine.upenn.edu,

Word count: 4389

References: 53

Figures: 6

Supplemental materials: 4 pages

Abstract

Objective. Ultraviolet B (UVB) is an important trigger of skin inflammation and lupus with recruitment of leukocytes to inflamed skin. Neutrophil NETosis has been implicated in pathogenesis of lupus erythematosus. We recently reported that nuclear envelope rupture and NET formation is driven by PKCα-mediated nuclear lamin B disassembly, with involvement of NETosis in UVB-induced skin inflammation. Studies have shown that cytoskeletal networks are involved in NETosis. However, it is still unknown how cytoskeletal networks and their upstream ROCK are involved in NET formation as well as UVB-induced skin inflammation.

Methods. The involvements of actomyosin cytoskeletal networks and ROCK1 in NETosis were studied in vitro. Mice with hematopoietic specific ROCK1 deficiency were irradiated by UVB to investigate NET formation in vivo and its involvement in skin inflammation.

Results. In time course studies, PKCα nuclear translocation was very well matched with actin polymerization and ROCK1 activation. Inhibition of actin polymerization or ROCK/MLCK/myosin pathway with chemical inhibitors decreased nuclear translocation of PKCα and NETosis *in vitro*. Furthermore, genetic deficiency of ROCK1 inhibited NET formation *ex vivo*. Hematopoietic specific ROCK1 deficiency ameliorated UVB-induced skin inflammation in mice with reduced skin thickness by attenuating NET formation and the extracellular display of NET-associated IL-17A, TNFα, IFNγ, and IFNα in the inflamed skin.

Conclusion. ROCK1 regulated neutrophils for NET formation by modulation of PKCα nuclear translocation through actomyosin cytoskeletal networks. ROCK1 deficiency ameliorates UVB-induced skin inflammation by inhibition of NETosis and display of NET-associated cytokines. This study provides insights into novel therapeutics on NETosis-related diseases.

INTRODUCTION

Ultraviolet B (UVB) is an important trigger of cutaneous and systemic lupus erythematosus (CLE, SLE) (1, 2). UVB overexposure causes photodamage of skin with recruitment of inflammatory cells, including neutrophils, monocytes and lymphocytes (3). A recent study has indicated that neutrophils are critical early infiltrating immune cells within cutaneous lupus lesion in mice (4). Several human studies with transcriptional profiling analysis of lupus patient samples also confirmed the importance of neutrophils (5), and a gradual enrichment of neutrophil transcripts during lupus disease progression (6). Therefore, it is important to understand the role of neutrophils in UVB-induced skin inflammation. NETosis is a unique form of neutrophil cell death with release neutrophil extracellular traps (NETs) (7). NETosis has been implicated in pathogenesis of lupus (8, 9). However, the involvement of NETosis in UVB-induced skin inflammation and the relevant cellular mechanisms has not been well understood.

Given that nuclear chromatin forms the backbone of NETs (7, 9), nuclear envelope rupture is required for chromatin release and extracellular NET formation. We recently found that NETotic nuclear envelope rupture is driven by protein kinase C (PKC)α-mediated phosphorylation and disassembly of nuclear lamin B (7), which is crucial to nuclear envelope integrity by forming highly organized meshworks surrounding the nuclear chromatin (10). Furthermore, cyclin-dependent kinases (CDK)4/6 also control NETosis through regulation of lamin A/C phosphorylation (11). Therefore, PKCα and CDK4/6 serve as NETotic lamin kinases (7, 11) to regulate nuclear lamina disassembly and nuclear envelope rupture.

PKCα exists diffusely in the cytosol of the unstimulated cells, but can be translocated to the nucleus during activation (12). Schmalz et al indicated that nuclear translocation of cytosolic

PKCα requires intact cytoskeleton (13). As a key cytoskeleton regulator, Rho kinase (ROCK) inhibition blocks intracellular translocation and activation of PKC (14). In the context of NETosis, we have shown that PKCα nuclear translocation is required for nuclear lamina disassembly and NET formation (7). Several studies also reported that NETosis induction in neutrophils also requires functional cytoskeleton (15-17). In the current study, we sought to study if cytoskeleton is involved in PKCα nuclear translocation during NETosis. Furthermore, F-actin and myosin motors form actin-myosin (actomyosin) cytoskeletal networks that are involved in nucleocytoplasmic shuttling (18). ROCK can regulate actomyosin cytoskeletal networks by activation of myosin II and myosin regulatory light chain kinase (MLCK) through the ROCK/MLCK/myosin pathway (19), and stabilize actin cytoskeleton filaments (20) through the ROCK/LIMK/Cofilin pathway (21). In the current study, we have investigated the effects of regulation of actin cytoskeleton filaments or actomyosin cytoskeletal networks by inhibition of ROCK/MLCK/ myosin pathway on PKCα nuclear translocation and NET formation in vitro. We have also studied the effects of genetic deficiency of ROCK1 on NETosis ex vivo. To explore the effects of ROCK1 deficiency on neutrophil NET formation in vivo and UVB-induced skin inflammation, we have generated mice with hematopoietic specific deficiency of ROCK1 by bone marrow transplantation (BMT).

METHODS

Mice. ROCK1 deficient mice ROCK1$^{+/-}$ on a C57BL/6J background were generated as prescribed before (22). C57BL/6J wildtype (WT) and CD45.1 (B6.SJL-*Ptprc*^{a}*Pepc*^{b}/BoyJ) mice

were purchased from Jackson Laboratory. All mice and their corresponding littermate controls were housed in a pathogen-free environment, and given food and water *ad libitum*. All animal experiments and animal protocols were approved by the Animal Care and Use Committee of University of Pennsylvania.

Cell Culture and Treatment. Primary human neutrophils or mouse bone marrow (BM) neutrophils from the *femur* and *tibia* BM from WT vs ROCK1$^{+/-}$ (22) were isolated as described in our publication (7). Mouse BM mPMNs were isolated from the *femur* and *tibia* BM with a neutrophil isolation kit (Miltenyl). Human HL-60 cell line were differentiated into polymorphic nuclear granulocytes (dPMNs) in RPMI-1640 with 10% FBS and 1.2% DMSO for 5-6 days as described in our published study (7). All of the above primary neutrophils or dPMNs were treated with, either the most commonly used NETosis inducer PMA at 50-100 nM, or the naturally occurring lipid mediator platelet-activating factor (PAF) at 5-10 µM, for 0-3h without or with 1h pretreatment with inhibitors of F-actin polymerization (Cytochalasin D), myosin light chain (MLC) kinase (ML7), myosin II (Blebbistatin), or ROCK (AS1892802, HA-1077, Y-27632), following by detection of NET formation, or lysis for immunoblot analysis. Relative transwell migration of BM neutrophils from WT vs ROCK1$^{+/-}$ mice was examined by treatment with CXCL-1 at 100 ng/ml, and detected using Boyden chamber with pore size of 3.0 µm. The pore transmigration ability was expressed as relative transmigration compared to that in neutrophils without treatment.

Generation of hematopoietic deficient mice by bone marrow transplantation (BMT), and UVB Exposure. see Supplementary materials on the *Arthritis & Rheumatology* website.

Assessment of NETs, actin polymerization, and ROCK activity. All of the above primary human or mouse neutrophils or dPMNs were treated with either PMA (50 or 100 nM) or *PAF* (5 or 10 μM) for 0-3h. NET formation assessment and quantification was analyzed by either conventional fluorometric NET quantification by SYTOX Green staining intensity, and/or immunofluorescent imaging quantification analysis by staining with impermeable DNA dye SYTOX Green (500 nM) for detection of NET formation, and the cell-permeable DNA dye SYTO Red to count the total number of cells, as described before (7). Time course treatment of dPMNs by 50 nM PMA for 5, 15, 30, 60, 120, and/or 180 min, then cells were either fixed or lysed with cell lysis buffer for different experiments. For detection of polymerized filamentous actin (F-actin), the 2% paraformaldehyde (PFA) fixed cells from different time points were stained by RFP-labeled phalloidin and analyzed with flow cytometry according to published method (23). For detection of ROCK activity, the cell lysates from different time points were analyzed with ROCK activity detection kit (Millipore).

Fluorescent Immunocytochemistry and Immunohistochemistry analysis. For immuno-cytochemistry analysis, dPMNs or mouse BM neutrophils were treated without or with different inhibitors, then treated without or with PMA or PAF for 1-3h for study of PKCα nuclear translocation. Then the treated cells were stained by primary anti-total PKCα or anti-lamin B Abs, followed by secondary Abs with FITC or PE conjugation (7). For the ex vivo NETosis induction with exhibition of NET-associated cytokines, the BM neutrophils from ROCK1$^{+/-}$ vs WT were treated overnight without or with PAF, without or with isolated NETs (for IFNα induction). Then the treated cells were fixed with 2% PFA and permeabilized with 0.1% Triton

X-100, and stained by primary antibodies against IL-17A, TNFα, IFNγ, or IFNα with FITC- or Alexa488-conjugation (Biolegend or Bioss). The neutrophil marker Alexa-647-labeled anti-ly6G was used. DNA was stained with DAPI.

The paraffin-embedded skin tissue sections were stained as described before (7). The neutrophil markers Alexa-647-labeled anti-ly6G were used for detection of neutrophils and NETosis in combination with DNA staining with DAPI as described (7). FITC- or Alexa488-conjugated primary antibodies against IL-17A, TNFα, IFNγ, or IFNα were used to stain cytokines (Biolegend or Bioss). Slides were mounted with Gold Antifade Mountant (Invitrogen). Confocal fluorescent images were analyzed with an Olympus Fluoview 1000 confocal microscope.

Statistical analyses. Prism 6 (GraphPad Software) was used to perform statistical analysis. Normally distributed data are shown as means ± standard deviations (SD). Comparisons between two groups were conducted with student T test. Comparisons amongst three or more groups were performed using ANOVA, followed by Student-Newman-Keuls test. Pearson correlation analysis was used when applicable. Comparison between two groups was analyzed using Student's t-test. Statistical significance was considered at a level of P-value < 0.05.

RESULTS

Disruption of actin cytoskeleton filaments or actomyosin cytoskeletal networks attenuate NETosis in neutrophils. Since nuclear envelope rupture and lamin B disassembly is mediated

by nuclear translocation of PKCα (7), a process that requires intact cytoskeleton (13, 17, 24), we examined the effects of the regulation of cytoskeletal networks on NETosis. We found that the disruption of actin cytoskeleton filaments by inhibition of actin polymerization with cytochalasin D, or disruption of actomyosin cytoskeletal networks by inhibition of myosin II with Blebbistatin or inhibition of the upstream MLCK with ML7, decreased PMA-induced NETosis in neutrophils (Figure 1A-C). Importantly, disruption of actin cytoskeleton filaments or inhibition of myosin II or MLCK blocked nuclear translocation of PKCα (Fig 1D), in which we saw that many PKCα molecules still remain in the cytosol and the nuclei still remain polymorphous (Fig 1D). In contrast, we saw the swelling nuclei with disintegrated nuclear envelope in cells treated with PMA alone (Fig 1D). Therefore, our studies demonstrated that not only actin cytoskeleton filaments, but also actomyosin cytoskeletal networks, are important for nuclear translocation of PKCα and nuclear envelope rupture (Fig 1E), which allow nuclear chromatin release and NET formation (7). Other studies also reported the involvement of actin cytoskeleton (25) or myosin II (26) in nuclear translocation of cytosolic molecules, as well as the role of actomyosin-dependent nucleocytoplasmic shuttling (18).

ROCK regulated PKCα nuclear translocation by regulation of actin polymerization in neutrophils. To study the effects of actin cytoskeleton filaments and their regulation by ROCK on PKCα nuclear translocation, a time course study with microscopic analysis (starting at 5 minutes to allow neutrophils to adhere on plates) showed that the diffusely distributed cytoplasmic PKCα gradually translocated into the nucleus from 15 to 60 minutes after PMA stimulation (Fig 2A), and subsequently induced nuclear lamin B disassembly and nuclear envelop disintegration at 60 min (Fig 2A). This made it possible for nuclear chromatin extrusion

from the ruptured site of the nuclear envelope and extracellular NET formation at a later time point (120 min, Fig 2A) (7). In parallel, we found that PMA induced a time-dependent increase of actin polymerization and F-actin filament formation at 15 and 30 min, reached a peak by 60 min, and then gradually decreased at 120 and 180 min (Fig 2B). A previous study also reported that PMA can induce actin polymerization in neutrophils (24). Importantly, the parallel changes of PKCα nuclear translocation and actin polymerization from 0 to 60 min (Fig 2A,B) support the previous findings for the role of actin cytoskeleton in PKCα nuclear translocation (13). Our results suggests that actin polymerization is important for nuclear translocation of PKCα, which serves as a NETotic lamin kinase to disassemble nuclear lamin B, resulting in nuclear envelope rupture. This provides the physical "door" for nuclear chromatin extrusion and NET formation.

In parallel with PMA-induced F-actin polymerization (Fig 2B), we also found a tightly matched time course of PMA-induced ROCK activation that appeared to be activated as early as 15 min, peaked at 60 min, and then gradually decreased at 2-3h time points (Fig 2C). Interestingly, the time course of PMA-induced actin polymerization (Fig 2B) and ROCK activation (Fig 2C) were very well matched with the process of PKCα nuclear translocation at 0-60 min, resulting in nuclear envelope disintegration at 60 min (Fig 2A). Importantly, inhibition of ROCK activation by pretreatment of neutrophils with ROCK inhibitors (Y27632, HA1077, AS1892802) not only alleviated PMA-induced actin polymerization (Fig 2D), but also attenuated PKCα nuclear translocation, and inhibited nuclear envelope disassembly, in which the nuclei of those cells remained polymorphous (Fig 2E). Therefore, PKCα nuclear translocation is mediated by not only the actin cytoskeleton (13), but also the upstream ROCK/MLCK/myosin pathway (Fig 1E,2E,2F). Our results provide a mechanistic explanation for the role of functional cytoskeleton and its regulation by ROCK in PKCα nuclear translocation, nuclear envelope

rupture, and NETosis induction (15-17). Other studies also reported the role of ROCK in nuclear translocation of cytoplasmic molecules through regulation of actin cytoskeleton (27).

Inhibition of ROCK1 by pharmacological inhibition or genetic deficiency attenuates NET formation in neutrophils *in vitro* or *ex vivo*. To explore the role of ROCK1 in NETosis, we found that inhibition of ROCK with different inhibitors (Y27632, HA1077, AS1892802) significantly decreased NET formation in vitro throughout a 3h time period in dPMNs (Fig 3A) and after 3 hours with primary neutrophils (Fig 3B,C). Most importantly, genetic deficiency of ROCK1 also inhibited NETosis ex vivo in BM neutrophils from ROCK1$^{+/-}$ mice as compared to those from their WT littermates (Fig 3D,E). Since the processes of ROCK activation (Fig 2C), actin polymerization (Fig 2B), and PKCα nuclear translocation (Fig 2A) were tightly matched in a time-dependent manner at 0-60 min, inhibition of ROCK attenuated actin polymerization (Fig 2D), or PKC nuclear accumulation (Fig 2E), and NETosis in vitro or ex vivo (Fig 3A-F), these results from in vitro and ex vivo experiments indicate that ROCK signal pathway regulates NETosis by modulation of nuclear translocation of the NETotic lamin kinase PKCα and nuclear lamina disintegration through regulation of actomyosin cytoskeletal networks.

Hematopoietic specific ROCK1 deficiency protects mice from UVB-induced skin inflammation. To study the effects of regulation of ROCK on controlling neutrophil NET formation in vivo and UVB-induced skin inflammation, we generated mice with hematopoietic specific ROCK1 deficiency by transplantation of HSCs from the BM of ROCK1$^{+/-}$ mice or their WT littermates to CD45.1 mice (Fig 4A). Four weeks after the BMT procedure, the reconstitution rate of donor-derived cells (CD45.2) in the peripheral blood of the recipient

CD45.1 mice was examined by flow cytometry for each mouse. Only the CD45.1 recipient mice with reconstitution rates over 95% (Fig 4B) were included for the next in vivo studies. The IHC staining of the infiltrated donor-derived neutrophils (CD45.2) and NET formation in skin lesions of UVB-irradiated CD45.1 recipient mice that received BMT of HSCs from WT donors (Fig 4C) further confirmed the successful BMT with high reconstitution. Importantly, the confocal image analysis demonstrated decreased NET formation *in vivo* in skin lesions of UVB-irradiated BMT-ROCK1$^{+/-}$ mice as compared to those of BMT-WT control mice (Fig 4D,E). Consequently, the skin thickness of both epidermis and dermis, as well as inflammatory cell infiltration in UVB-irradiated BMT-ROCK1$^{+/-}$ mice were decreased as compared to those in BMT-WT control mice (Fig 4F-I). Infiltration of inflammatory cells in the skin was correlated with skin thickness of dermis in all experimental mice (Suppl Fig 1A). These results indicate that hematopoietic-specific ROCK1 deficiency protects mice from UVB-induced skin inflammation.

To understand the decreased neutrophils with NET formation in the skin of UVB-irradiated ROCK1 deficient mice, we conducted cell transmigration experiments of neutrophils from these mice as ROCK1 is known to modulate actin cytoskeleton that is involved in cell migration (28). Wang et al reported that macrophages from ROCK1$^{-/-}$ mice showed significantly impaired chemotactic responses (28). In the current study we found mild but significant decreases in chemotactic migration responses in neutrophils from ROCK1$^{+/-}$ mice as compared to those from WT mice (Suppl Fig 1B). These results indicate that ROCK1 deficiency in neutrophils may affect cell migration (Suppl Fig 1B). However, we still see that many diffusely distributed neutrophils infiltrated to skin of UVB-irradiated BMT-ROCK1$^{+/-}$ mice (Fig 4E,F). Therefore, the attenuated skin inflammation cannot be explained by the mild decrease in chemotactic migration of ROCK1 deficient neutrophils in ROCK1$^{+/-}$ mice (Fig 4F-I). Other factors, i.e. chemotactic

effects of NET-associated cytokines may also contribute to leukocyte infiltration as our recent publication demonstrates that NETs can display IL-17A and TNFα (7), proinflammatory cytokines that are known to contribute to the recruitment of inflammatory cells in various contexts (29).

Hematopoietic-specific ROCK1 deficiency decreased the exhibition of pro-inflammatory cytokines by neutrophil NETs in BMT-ROCK1$^{+/-}$ mice. To further study NET-related inflammation, we found that UVB exposure increased formation of NETs that exhibit proinflammatory cytokines IL-17A, TNFα, IFNγ, or IFNα in the inflamed skin of BMT-WT mice (Fig 5A-I), while hematopoietic-specific ROCK1 deficiency can ameliorate skin inflammation through inhibition of NET formation in vivo and attenuate the display of NET-associated cytokines in UVB-irradiated skin of BMT-ROCK1$^{+/-}$ mice (Fig 5A-I). Many cytokines have chemotactic properties for recruitment of inflammatory cells (29-31). Here, we found NET-associated IL-17A or TNFα in the inflamed skin, while IL-17A (30) together with TNFα (31) are known to synergistically induce leukocyte infiltration to the sites of inflammation (32). Furthermore, NET-associated IFNγ together with IL-17A also promote leukocyte recruitment (29). Thus, the display of NET-associated IL-17A, TNFα, and IFNγ contribute to the leukocyte recruitment and their accumulation in certain areas of the dermis, as well as propagation of inflammatory responses in the inflamed skin of UVB-irradiated BMT-WT mice (Fig 4E, 5C). However, there were not only fewer, but also diffusely distributed leukocytes in the skin of UVB-irradiated BMT-ROCK1$^{+/-}$ mice (Fig 4E, 5C). In UVB-irradiated BMT-WT mice, the NET-associated cytokines were distributed locally with a relatively high concentration in the extracellular matrix. This likely contributes to the accumulation of leukocytes in the skin of

BMT-WT mice. In contrast, the non-netting neutrophils may secrete their cytokines that quickly diffuse to the blood stream and are then diluted by the circulation. This may partly contribute to the decreased leukocyte infiltration and accumulation in the skin of UVB-irradiated BMT-ROCK1$^{+/-}$ mice (Fig 4E, 5C). In addition to the above cytokines, we also detected NET-associated IFNα, an important cytokine that not only contributes to the inflammatory response, but is also implicated in the autoimmune response in the context of lupus and photosensitivity after UVB irradiation in patients with lupus.

ROCK1 genetic deficiency inhibited formation of NETs *ex vivo* and their exhibition of pro-inflammatory cytokines in neutrophils from ROCK1 deficient mice. Published studies have reported that neutrophils can express and produce various cytokines, including IL-17A (29), TNFα (33), IFNγ (34), or IFNα (35). These neutrophil-expressed cytokines can be released with NETs (35). Recently, Agak et al reported that extracellular traps released by TH17 cells can also be associated with IL-17 (36). In the current study, we found the display of NET-associated cytokines in UVB-irradiated skin (Fig 5). To determine if these NET-associated cytokines were derived from their parental neutrophils, we conducted ex vivo experiments by treatment of mouse neutrophils with PAF, a natural lipid mediator release by keratinocytes after UVB exposure (7). We found that the NETs from the PAF-stimulated WT neutrophils can also display IL-17A, TNFα, and IFNγ in the extracellular space with their extracellular NET structure (Fig 6A,C,E). In contrast, ROCK1 deficiency attenuated NET formation and the above cytokines were enclosed within the non-netting ROCK1$^{+/-}$ neutrophils in relative smaller area (Fig 6B,D,F). In addition, we also found IFNα expression in neutrophils and its extracellular display with NETs in WT neutrophils that treated with both PAF and isolated DNA NETs (NET+PAF), while

ROCK1 deficiency reduced the NET formation and IFNα was enclosed within the non-netting ROCK1$^{+/-}$ neutrophils in relative smaller area. Therefore, with stimulation by PAF released from skin keratinocytes of UVB-irradiated mice, the recruited neutrophils can form NETs that exhibit proinflammatory cytokines in local skin, which further recruited neutrophils, thus resulting in increased leukocyte recruitment and accumulation in certain area, particularly the epidermal-dermal junction area of the inflamed skin. In contrast, inhibition of NET formation by ROCK1 deficiency resulted in the intracellular retention of those cytokines, attenuating their display by extracellular NETs and resulting in fewer and diffusely distributed leukocytes in the skin, thus ameliorating UVB-induced skin inflammation.

DISCUSSION

Photosensitive skin reaction is a complex inflammatory response to UVB-induced tissue damage. It is already over half century since the role of UVB in lupus was reported, however the relevant mechanisms are still not well understood. UVB overexposure causes epidermal keratinocyte apoptosis and DNA damage (37, 38). Accumulation of dead cell extracellular DNA may initiate autoimmune responses and contribute to lupus development (39). However, some studies questioned the role of UVB-induced keratinocyte apoptosis in lupus development (40). Beyond apoptosis, other types of cell death have also contributed to extracellular DNA accumulation and autoimmunity as well as lupus development (41). Histopathologic analysis of lupus skin indicates the potential interaction of between immune cell-epidermal keratinocytes (39, 42). UVB irradiation of keratinocytes releases PAF, which contributes to the sustained inflammatory responses (43) and induces recruitment of neutrophils to the damaged skin. There,

PAF may further induce NETosis of the recruited neutrophils in UVB-irradiated skin (7). Studies (7) have shown that PAF may serve as a natural stimulus for NETosis induction. On the other hand, studies from our group and others have shown that UV exposure can induce neutrophil NET formation *in vitro* (7, 44). Therefore, neutrophil NET formation *in vivo* in UVB-irradiated skin may be attributed to both indirect effects of UVB by PAF (43) and direct effects of UVB irradiation (7, 44) on neutrophils in the inflamed skin.

We have reported that NETotic nuclear envelope rupture and chromatin extracellular release is driven by PKCα-mediated phosphorylation and disassembly of nuclear lamin B (7). This mechanism is also suited to explain the in vivo NET formation in skin in the context of UVB irradiation with either PAF stimulation or direct UVB exposure of neutrophils as we have experimentally addressed (7). Therefore, nuclear translocation of cytosolic PKCα (7, 12) by the actin cytoskeleton (13) or actomyosin cytoskeletal networks investigated in the current study is an important step. In the current study, we found that either disruption of actin cytoskeleton filaments by direct inhibition of actin cytoskeleton polymerization, or regulation of actomyosin cytoskeletal networks by inhibition of the ROCK/MLCK/myosin signaling pathway with either chemical inhibitors or genetic ROCK1 deficiency can attenuate NET formation through interfering with nuclear translocation of NETotic lamin kinase PKCα. Several previous studies have reported that NETosis induction requires functional cytoskeleton (15, 17), and genetic disruption of actin polymerization by a deficiency of Wiskott-Aldrich syndrome protein blocks NET formation (16). The current study thus provides a potential cellular mechanistic explanation for the role of actin cytoskeleton in NETosis.

In line with our findings, other studies also report the involvement of actin cytoskeleton filament (25), or myosin II (26), or actomyosin-dependent (18) nucleocytoplasmic shuttling.

Furthermore, studies also reported the role of ROCK in nuclear translocation of cytoplasmic molecules through regulation of the actin cytoskeleton (45). Therefore, the current study, along with previous studies, suggests that actomyosin cytoskeletal networks may serve as a "transportation system" for nuclear translocation of NETotic lamin kinase PKCα (13), which phosphorylates and disassembles nuclear lamina, resulting in nuclear envelope rupture. In addition to their role in nuclear-cytoplasmic shuttling (18), ROCK and its-regulated actomyosin cytoskeletal networks may also enable nuclear deformation and contribute to nuclear envelope rupture by the forces generated by the cytoskeletal networks (46). However, it is still unclear if actomyosin cytoskeletal networks also contribute to nuclear envelope rupture by tearing the disassembled nuclear lamina with their "forces". Furthermore, the cortical cytoskeletal networks are beneath the plasma membrane and both are linked through binding proteins (47). The contractile forces generated by cortical cytoskeletal networks are important for the maintenance of plasma membrane integrity (47). Recently, Thiam et al reported that disassembly of the cortical cytoskeleton in the late stages of NETosis may be responsible for the rupture of the plasma membrane in NETotic neutrophils (48). Therefore, the increased ROCK activity with enhanced actin polymerization at an early stage is necessary for nuclear translocation of PKCα which disassembles the nuclear lamina and ruptures the nuclear envelope, allowing the extrusion of nuclear chromatin. The decreased ROCK activity with reduced actin polymerization during the late stages of NETosis may contribute to plasma membrane rupture and extracellular release of chromatin and NET formation. In addition to the intracellular effects of ROCK-regulated acomyosin networks on PKCα nuclear translocation, actin cytoskeletal networks also regulate cell movement. Wang and colleagues demonstrated that macrophages with ROCK1 deletion from ROCK1$^{-/-}$ mice showed significantly impaired chemotactic responses (28). In the current

study, the ROCK1 deficient neutrophils from ROCK1$^{+/-}$ mice showed mildly decreased transmigration capability ex vivo in transwell experiments. In vivo, the UVB irradiated ROCK1$^{+/-}$ mice showed the mildly reduced leukocyte infiltration with a diffuse distribution in skin, suggesting the residual ROCK1 expression in leukocytes of ROCK1$^{+/-}$ mice (22) can still partly regulate actomyosin cytoskeletal networks to drive cell movement.

Our published study has demonstrated the involvement of NETs and NET-associated cytokines in UVB-induced skin inflammation (7). Ongusaha et al reported a role for ROCK in UVB-induced skin keratinocyte apoptosis (37). To address the role of neutrophils, we generated mice with hematopoietic specific ROCK1 deficiency. Similar to what we discussed above in vitro and ex vivo experiments as well as our recent publication (7), ROCK1 deficiency can decrease NET formation and the display of NET-associated cytokines in vivo in UVB-irradiated skin. The decreased extracellular exhibition of NET-associated IL-17A, TNFα, and IFNγ may be important for the reduced inflammatory cell infiltration and accumulation in UVB-irradiated skin, as IL-17A vs TNFα are known to synergistically sustain neutrophil recruitment to the sites of inflammation (32). IL-17A can also work with IFNγ to promote neutrophil recruitment (29) to inflamed skin. In contrast to the secreted cytokines that can diffuse freely to the circulation, the NET-associated cytokines can remain in the local skin at a relatively high concentration for a longer period of time, thus sustaining and propagating inflammatory responses in UVB-irradiated skin. Our recent publication demonstrated that blockage of TNFα with anti-TNFα significantly inhibited UVB-induced recruitment of inflammatory cells (49). Using mice with genetic deficiency, Li et al reported that both IL-17A and IFN-γ can be produced by neutrophils and may positively regulate neutrophil transmigration to the site of inflammation (29). All of the

above support the role of NET-associated IL-17A, TNFα, or IFNγ in the recruitment of inflammatory cells to the inflamed skin of UVB irradiated BMT-WT mice, while the reduced neutrophil NET formation with decreased extracellular display of NET-associated cytokines may partly explain the attenuated recruitment and accumulation of leukocytes in the inflamed skin of BMT-ROCK1$^{+/-}$ mice.

In addition to the above discussed chemotactic capability by cytokines presented by NETs, NET-associated IFNγ and IFNα not only contribute to UVB-induced skin inflammation (38, 50), but are also implicated in lupus (51-53). Although plasmacytoid dendritic cells are known to be professional cells for IFNα production, recent studies indicate that neutrophils may also express IFNα in the presence of chromatin (35). In the current study, we found NETotic neutrophils express IFNα in UVB-irradiated skin, probably triggered by chromatin released from nearby NETotic neutrophils. This is also confirmed by our ex vivo experiments in which we saw IFNα expression in neutrophils when they were stimulated by PAF and isolated NETs. Since type I interferon is a major driver of lupus, our results suggest that NETs and their associated IFNα may contribute to photosensitivity in lupus.

Taken together, ROCK1 regulated NET formation in neutrophils by modulation of nuclear translocation of PKCα through actomyosin cytoskeletal networks. ROCK1 deficiency ameliorates UVB-induced skin inflammation by attenuation of NET formation and display of NET-associated cytokines. This study helps explain the photosensitivity in lupus and the contribution of NETosis in UVB-induced skin inflammation. These findings provide insights into novel therapeutics in NETosis-related human diseases, including lupus.

AUTHOR CONTRIBUTIONS

Liu conceived and designed the study. Li, Lyu, Liu performed the laboratory experiments and acquired the experimental data. For the microscopic image analysis, Liu, Lyu, Li took the images, Lyu and Li conducted further quantification and statistical analysis. Liu, Lyu, and Werth analyzed and interpreted the data and finalized the paper. Li, Lyu, Liao, Werth and Liu were involved in preparation and revision of the manuscript. All authors read and approved the final manuscript.

ACKNOWLEDGEMENTS

The authors would like to acknowledge Penn Skin Biology and Diseases Resource-based Center for their skin histology service. The authors would thank Debra A. Pawlowski (animal facility, Philadelphia VA Medical Center) for her kindly help with our animal experiments. This work was supported by Lupus Research Alliance (416805) and NIH R21AI144838 (to Liu), the Veterans Affairs Merit Review Award (to Werth), and NIH HL052233 and HL136962 (to Liao).

CONFLICT OF INTEREST

The authors have no conflict of interests to declare.

References

1. Werth VP, Bashir M, and Zhang W. Photosensitivity in rheumatic diseases. *The journal of investigative dermatology Symposium proceedings / the Society for Investigative Dermatology, Inc.* 2004;9(1):57-63.
2. Deng GM, and Tsokos GC. Pathogenesis and targeted treatment of skin injury in SLE. *Nat Rev Rheumatol.* 2015;11(11):663-9.
3. Rodero MP, Handoko HY, Villani RM, Walker GJ, and Khosrotehrani K. Differential effects of ultraviolet irradiation in neonatal versus adult mice are not explained by defective macrophage or neutrophil infiltration. *The Journal of investigative dermatology.* 2014;134(7):1991-7.
4. Han X, Vesely MD, Yang W, Sanmamed MF, Badri T, Alawa J, Lopez-Giraldez F, Gaule P, Lee SW, Zhang JP, et al. PD-1H (VISTA)-mediated suppression of autoimmunity in systemic and cutaneous lupus erythematosus. *Science translational medicine.* 2019;11(522).
5. Panousis NI, Bertsias GK, Ongen H, Gergianaki I, Tektonidou MG, Trachana M, Romano-Palumbo L, Bielser D, Howald C, Pamfil C, et al. Combined genetic and transcriptome analysis of patients with SLE: distinct, targetable signatures for susceptibility and severity. *Annals of the rheumatic diseases.* 2019;78(8):1079-89.
6. Banchereau R, Hong S, Cantarel B, Baldwin N, Baisch J, Edens M, Cepika AM, Acs P, Turner J, Anguiano E, et al. Personalized Immunomonitoring Uncovers Molecular Networks that Stratify Lupus Patients. *Cell.* 2016;165(3):551-65.
7. Li Y, Li M, Weigel B, Werth VP, Mall M, and Liu ML. Nuclear envelope rupture and NET formation is driven by PKCα-mediated lamin B disassembly. *EMBO reports.* 2020;21(e48779).
8. Kahlenberg JM, Carmona-Rivera C, Smith CK, and Kaplan MJ. Neutrophil extracellular trap-associated protein activation of the NLRP3 inflammasome is enhanced in lupus macrophages. *J Immunol.* 2013;190(3):1217-26.
9. Lood C, Blanco LP, Purmalek MM, Carmona-Rivera C, De Ravin SS, Smith CK, Malech HL, Ledbetter JA, Elkon KB, and Kaplan MJ. Neutrophil extracellular traps enriched in oxidized mitochondrial DNA are interferogenic and contribute to lupus-like disease. *Nature medicine.* 2016;22(2):146-53.
10. Goldberg MW, Huttenlauch I, Hutchison CJ, and Stick R. Filaments made from A- and B-type lamins differ in structure and organization. *Journal of cell science.* 2008;121(Pt 2):215-25.
11. Amulic B, Knackstedt SL, Abu Abed U, Deigendesch N, Harbort CJ, Caffrey BE, Brinkmann V, Heppner FL, Hinds PW, and Zychlinsky A. Cell-Cycle Proteins Control Production of Neutrophil Extracellular Traps. *Developmental cell.* 2017;43(4):449-62.
12. Zauli G, Visani G, Bassini A, Caramelli E, Ottaviani E, Bertolaso L, Bertagnolo V, Borgatti P, and Capitani S. Nuclear translocation of protein kinase C-alpha and -zeta isoforms in HL-60 cells induced to differentiate along the granulocytic lineage by all-trans retinoic acid. *British journal of haematology.* 1996;93(3):542-50.
13. Schmalz D, Kalkbrenner F, Hucho F, and Buchner K. Transport of protein kinase C alpha into the nucleus requires intact cytoskeleton while the transport of a protein containing a canonical nuclear localization signal does not. *Journal of cell science.* 1996;109 (Pt 9)(2401-6.

14. Hippenstiel S, Kratz T, Krull M, Seybold J, von Eichel-Streiber C, and Suttorp N. Rho protein inhibition blocks protein kinase C translocation and activation. *Biochemical and biophysical research communications.* 1998;245(3):830-4.
15. Neeli I, Dwivedi N, Khan S, and Radic M. Regulation of extracellular chromatin release from neutrophils. *J Innate Immun.* 2009;1(3):194-201.
16. Stojkov D, Amini P, Oberson K, Sokollik C, Duppenthaler A, Simon HU, and Yousefi S. ROS and glutathionylation balance cytoskeletal dynamics in neutrophil extracellular trap formation. *The Journal of cell biology.* 2017;216(12):4073-90.
17. Liu ML. Functional actin cytoskeleton is required in early stage of NETosis induction. *Proceedings of the National Academy of Sciences of the United States of America.* 2020;117(37):22653-4.
18. Alisafaei F, Jokhun DS, Shivashankar GV, and Shenoy VB. Regulation of nuclear architecture, mechanics, and nucleocytoplasmic shuttling of epigenetic factors by cell geometric constraints. *Proceedings of the National Academy of Sciences of the United States of America.* 2019;116(27):13200-9.
19. Somlyo AP, and Somlyo AV. Ca2+ sensitivity of smooth muscle and nonmuscle myosin II: modulated by G proteins, kinases, and myosin phosphatase. *Physiological reviews.* 2003;83(4):1325-58.
20. Gallo RM, Khan MA, Shi J, Kapur R, Wei L, Bailey JC, Liu J, and Brutkiewicz RR. Regulation of the actin cytoskeleton by Rho kinase controls antigen presentation by CD1d. *J Immunol.* 2012;189(4):1689-98.
21. Lin T, Zeng L, Liu Y, DeFea K, Schwartz MA, Chien S, and Shyy JY. Rho-ROCK-LIMK-cofilin pathway regulates shear stress activation of sterol regulatory element binding proteins. *Circulation research.* 2003;92(12):1296-304.
22. Rikitake Y, Oyama N, Wang CY, Noma K, Satoh M, Kim HH, and Liao JK. Decreased perivascular fibrosis but not cardiac hypertrophy in ROCK1+/- haploinsufficient mice. *Circulation.* 2005;112(19):2959-65.
23. Cano ML, Cassimeris L, Fechheimer M, and Zigmond SH. Mechanisms responsible for F-actin stabilization after lysis of polymorphonuclear leukocytes. *The Journal of cell biology.* 1992;116(5):1123-34.
24. Downey GP, Chan CK, Lea P, Takai A, and Grinstein S. Phorbol ester-induced actin assembly in neutrophils: role of protein kinase C. *The Journal of cell biology.* 1992;116(3):695-706.
25. Yamamura S, Goda N, Akizawa H, Kohri N, Balboula AZ, Kobayashi K, Bai H, Takahashi M, and Kawahara M. Yes-associated protein 1 translocation through actin cytoskeleton organization in trophectoderm cells. *Developmental biology.* 2020;468(1-2):14-25.
26. Thomas DG, Yenepalli A, Denais CM, Rape A, Beach JR, Wang YL, Schiemann WP, Baskaran H, Lammerding J, and Egelhoff TT. Non-muscle myosin IIB is critical for nuclear translocation during 3D invasion. *The Journal of cell biology.* 2015;210(4):583-94.
27. Matoba K, Kawanami D, Tsukamoto M, Kinoshita J, Ito T, Ishizawa S, Kanazawa Y, Yokota T, Murai N, Matsufuji S, et al. Rho-kinase regulation of TNF-alpha-induced nuclear translocation of NF-kappaB RelA/p65 and M-CSF expression via p38 MAPK in mesangial cells. *Am J Physiol Renal Physiol.* 2014;307(5):F571-80.

28. Wang HW, Liu PY, Oyama N, Rikitake Y, Kitamoto S, Gitlin J, Liao JK, and Boisvert WA. Deficiency of ROCK1 in bone marrow-derived cells protects against atherosclerosis in LDLR-/- mice. *FASEB J.* 2008;22(10):3561-70.
29. Li L, Huang L, Vergis AL, Ye H, Bajwa A, Narayan V, Strieter RM, Rosin DL, and Okusa MD. IL-17 produced by neutrophils regulates IFN-gamma-mediated neutrophil migration in mouse kidney ischemia-reperfusion injury. *The Journal of clinical investigation.* 2010;120(1):331-42.
30. Roussel L, Houle F, Chan C, Yao Y, Berube J, Olivenstein R, Martin JG, Huot J, Hamid Q, Ferri L, et al. IL-17 promotes p38 MAPK-dependent endothelial activation enhancing neutrophil recruitment to sites of inflammation. *J Immunol.* 2010;184(8):4531-7.
31. Smart SJ, and Casale TB. Pulmonary epithelial cells facilitate TNF-alpha-induced neutrophil chemotaxis. A role for cytokine networking. *J Immunol.* 1994;152(8):4087-94.
32. Griffin GK, Newton G, Tarrio ML, Bu DX, Maganto-Garcia E, Azcutia V, Alcaide P, Grabie N, Luscinskas FW, Croce KJ, et al. IL-17 and TNF-alpha sustain neutrophil recruitment during inflammation through synergistic effects on endothelial activation. *J Immunol.* 2012;188(12):6287-99.
33. Hilda JN, and Das SD. TLR stimulation of human neutrophils lead to increased release of MCP-1, MIP-1alpha, IL-1beta, IL-8 and TNF during tuberculosis. *Human immunology.* 2016;77(1):63-7.
34. Yamada M, Gomez JC, Chugh PE, Lowell CA, Dinauer MC, Dittmer DP, and Doerschuk CM. Interferon-gamma production by neutrophils during bacterial pneumonia in mice. *American journal of respiratory and critical care medicine.* 2011;183(10):1391-401.
35. Lindau D, Mussard J, Rabsteyn A, Ribon M, Kotter I, Igney A, Adema GJ, Boissier MC, Rammensee HG, and Decker P. TLR9 independent interferon alpha production by neutrophils on NETosis in response to circulating chromatin, a key lupus autoantigen. *Annals of the rheumatic diseases.* 2013.
36. Agak GW, Mouton A, Teles RM, Weston T, Morselli M, Andrade PR, Pellegrini M, and Modlin RL. Extracellular traps released by antimicrobial TH17 cells contribute to host defense. *The Journal of clinical investigation.* 2021;131(2).
37. Ongusaha PP, Qi HH, Raj L, Kim YB, Aaronson SA, Davis RJ, Shi Y, Liao JK, and Lee SW. Identification of ROCK1 as an upstream activator of the JIP-3 to JNK signaling axis in response to UVB damage. *Science signaling.* 2008;1(47):ra14.
38. Wolf SJ, Estadt SN, Gudjonsson JE, and Kahlenberg JM. Human and Murine Evidence for Mechanisms Driving Autoimmune Photosensitivity. *Frontiers in immunology.* 2018;9(2430.
39. Sim JH, Ambler WG, Sollohub IF, Howlader MJ, Li TM, Lee HJ, and Lu TT. Immune Cell-Stromal Circuitry in Lupus Photosensitivity. *J Immunol.* 2021;206(2):302-9.
40. Reefman E, de Jong MC, Kuiper H, Jonkman MF, Limburg PC, Kallenberg CG, and Bijl M. Is disturbed clearance of apoptotic keratinocytes responsible for UVB-induced inflammatory skin lesions in systemic lupus erythematosus? *Arthritis research & therapy.* 2006;8(6):R156.
41. Colonna L, Lood C, and Elkon KB. Beyond apoptosis in lupus. *Current opinion in rheumatology.* 2014;26(5):459-66.
42. Kahlenberg JM. Rethinking the Pathogenesis of Cutaneous Lupus. *The Journal of investigative dermatology.* 2020.

43. Damiani E, and Ullrich SE. Understanding the connection between platelet-activating factor, a UV-induced lipid mediator of inflammation, immune suppression and skin cancer. *Progress in lipid research.* 2016;63(14-27.
44. Zawrotniak M, Bartnicka D, and Rapala-Kozik M. UVA and UVB radiation induce the formation of neutrophil extracellular traps by human polymorphonuclear cells. *J Photochem Photobiol B.* 2019;196(111511.
45. Liu Y, Suzuki YJ, Day RM, and Fanburg BL. Rho kinase-induced nuclear translocation of ERK1/ERK2 in smooth muscle cell mitogenesis caused by serotonin. *Circulation research.* 2004;95(6):579-86.
46. Wesolowska N, Avilov I, Machado P, Geiss C, Kondo H, Mori M, and Lenart P. Actin assembly ruptures the nuclear envelope by prying the lamina away from nuclear pores and nuclear membranes in starfish oocytes. *Elife.* 2020;9(
47. Chugh P, and Paluch EK. The actin cortex at a glance. *Journal of cell science.* 2018;131(14).
48. Thiam HR, Wong SL, Qiu R, Kittisopikul M, Vahabikashi A, Goldman AE, Goldman RD, Wagner DD, and Waterman CM. NETosis proceeds by cytoskeleton and endomembrane disassembly and PAD4-mediated chromatin decondensation and nuclear envelope rupture. *Proceedings of the National Academy of Sciences of the United States of America.* 2020;117(13):7326-37.
49. Sharma MR, Mitrani R, and Werth VP. Effect of TNFalpha blockade on UVB-induced inflammatory cell migration and collagen loss in mice. *J Photochem Photobiol B.* 2020;213(112072.
50. Skopelja-Gardner S, An J, Tai J, Tanaka L, Sun X, Hermanson P, Baum R, Kawasumi M, Green R, Gale M, Jr., et al. The early local and systemic Type I interferon responses to ultraviolet B light exposure are cGAS dependent. *Sci Rep.* 2020;10(1):7908.
51. Seery JP. IFN-gamma transgenic mice: clues to the pathogenesis of systemic lupus erythematosus? *Arthritis Res.* 2000;2(6):437-40.
52. Sarkar MK, Hile GA, Tsoi LC, Xing X, Liu J, Liang Y, Berthier CC, Swindell WR, Patrick MT, Shao S, et al. Photosensitivity and type I IFN responses in cutaneous lupus are driven by epidermal-derived interferon kappa. *Annals of the rheumatic diseases.* 2018.
53. Oke V, Gunnarsson I, Dorschner J, Eketjall S, Zickert A, Niewold TB, and Svenungsson E. High levels of circulating interferons type I, type II and type III associate with distinct clinical features of active systemic lupus erythematosus. *Arthritis research & therapy.* 2019;21(1):107.

Figure Legends

Figure 1. Disruption of actin cytoskeleton filaments or actomyosin cytoskeletal networks attenuates NETosis in neutrophils. In panels **A-C**, dPMNs (**A**) or primary (**B**,**C**) human neutrophils were exposed to 50 nM PMA without or with pretreatment by Cytochalasin D (Cyto D), Blebbistatin, or ML7, then detection of NETosis by Sytox Green staining, after 1h, 2h, and 3h of PMA treatment for dPMNs (**A**), or after 3h treatment for primary neutrophils (**B**,**C**), by microplate reader (**A**,**B**) or by fluorescent microscopy (**C**). Scale bar, 50 μm. **D**. Effects of Cyto D, Blebbistatin, and ML7 on nuclear translocation of PKCα and lamina (lamin B) disintegration in dPMNs exposed to 50 nM PMA for 60 min without or with 30 min pretreatment by above inhibitors, then stained for **lamin B** and **PKCα** with corresponding antibodies. Allows indicate the disintegration/rupture of the nuclear envelope (**D**). Scale bars, 10 μm. Panel **E** displays the schematic illustration of the involvement of actin cytoskeleton filaments, actomyosin cytoskeletal networks in NETosis and the corresponding inhibitors. Panels **A**,**B** display means±SEM. For panel **A**, the comparisons were among control and PMA treatment groups at 1h, 2h, and 3h respectively. P**<0.01, P***<0.001 vs controls, while P††<0.01, P†††<0.001 vs PMA treated groups. All results are representative of 3 or more experiments. Panels **B**,**C** were only for 3h PMA, P<0.01 by ANOVA; displayed are significance levels for individual pairwise comparisons by the Student-Newman Keuls test.

Figure 2. PKCα nuclear translocation and actin cytoskeleton assembly were regulated by Rho kinase 1 (ROCK1). Panel **A,** Time course of PKCα nuclear translocation, subsequent lamin B disassembly and nuclear lamina disintegration, and NET release in dPMNs exposed to 50 nM

PMA for 0-120 min, then stained simultaneously for **DNA**, **lamin B** (probed by primary anti-lamin B, and FITC-labeled secondary antibody), and **PKCα** (primary anti-PKCα, and PE-labeled secondary antibody) under confocal fluorescent microscopy. Panel **B**, Time course of F-actin polymerization in dPMNs exposed to 50 nM PMA for 0-180 min, the pemeabilized cells were probed with phalloidin-RFP and detected by flow cytometry. Scale bars, 10 μm. Panel **C** shows the time course of ROCK activation in dPMNs exposed to 50 nM PMA for 0-180 min, detected by ROCK activity ELISA. Panel **D** indicates F-actin polymerization detected by RFP-labeled phalloidin with flow cytometry in dPMNs exposed to 50 nM PMA for 60 min without or with 30 min pretreatment by different ROCK inhibitors (Y27632, HA1077, AS1892802). Panel **E**, Effect of ROCK inhibitors on PKCα nuclear translocation and nuclear envelope disassembly in dPMNs exposed to PMA for 60 min without or with 30 min pretreatment by ROCK inhibitors, then stained for **lamin B** and **PKCα** with corresponding Abs as Fig 1. Scale bar, 10 μm. Light blue arrows in panels **A**,**E** indicate the disintegration/rupture of nuclear lamina, while white arrows (**A**) indicate the rupture site of the nuclear envelope where the decondensed chromatin releases for NET formation. Panel **F** displays the schematic illustration of the involvement of actin cytoskeleton filaments, actomyosin cytoskeletal networks, their upstream signaling pathways, and ROCK, as well as their corresponding inhibitors in NETosis. All results are representative of 3 or more independent experiments. Panels A,B,D,E are the representative from three independent experiments. P**<0.01, P***<0.001 vs 0h in panel C from three independent experiments.

Figure 3. Inhibition of ROCK1 by pharmacological inhibitors or genetic deficiency attenuates NETosis in neutrophils. Panels **A-C** show the results of NETosis of dPMNs (**A**) or primary

neutrophils (**B**,**C**) that were exposed to 50 nM PMA for 1-3h without or with 30min pretreatment by ROCK inhibitors (Y27632, HA1077, AS1892802), then detection of NET formation after 1-3h of PMA treatment in dPMNs (**A**), or after 3h treatment in primary neutrophils (**B**,**C**), by microplate reader (A,B) or by fluorescent microscopy (**C**). Scale bars, 50μm. (**D**) Summary analysis and (**E**) representative of NET formation of mouse BM neutrophils from WT vs ROCK1$^{+/-}$ mice stimulated without or with 10 μM PAF for 3h, and stained with cell permeable SYTO Red and cell impermeable Sytox Green, without fixation. Images were taken by confocal microscopy, followed by automated quantification of NETs in 5-6 non-overlapping areas per well using ImageJ for calculation of % cells with NET formation. All results are representative of 3 or more independent experiments. Panels C,E are representative images from three or more independent experiments. Scale bars, 100μm. Panels A,B,D display mean±SEM. For panel **A,** the comparisons were among control and PMA treatment groups at 1h, 2h, and 3h respectively. P**<0.01, P***<0.001 vs controls, while P†<0.05, P†††<0.001 vs PMA treated groups. Panels B-E are only for 3h PMA or PAF treatment. In these panels, P< 0.01 by ANOVA; displayed are significance levels for individual pairwise comparisons by the Student-Newman Keuls test.

Figure 4. Hematopoietic specific ROCK1 deficiency protected mice from UVB-induced skin inflammation in BMT-ROCK1$^{+/-}$ mice. Panel **A** displays the experimental design for generation of hematopoietic specific BMT-ROCK1$^{+/-}$ mice by BMT, and grouping for UVB exposure. **B**, representative of flow cytometry analysis from all experimental mice for detection of reconstitution rate of donor-derived cells (CD45.2) in peripheral blood of recipient mice (CD45.1). **C**. The representative image of immunohistochemistry staining of skin lesion from UVB-irradiated CD45.1 recipient mice with BMT of HSCs from WT donors, stained by

antibodies against **Ly6G** (PE), **CD45.2** (FITC) or **DAPI**. Arrows indicate the reconstituted neutrophils that were infiltrated to the inflamed skin of recipient mice with UVB irradiation. **D,E,** representative and summary analysis of NETosis in skin of MT-WT vs BMT-ROCK1$^{+/-}$ mice that were irradiated without (sham) or with UVB, and skin sections were stained by antibodies against **Ly6G** (PE) and **DAPI**. **F-I**. Representative H&E images (**F**) and summary analysis of the thickness of epidermis and dermis (**G,H**), and infiltration of inflammatory (nucleated) cells in the dermis and subcutaneous fat layer (**I**) based on H&E staining of skin sections of BMT-WT vs BMT-ROCK1$^{+/-}$ mice that were irradiated without (sham) or with UVB. In the panels E,G,H,I, P<0.01 by ANOVA; displayed are significance levels for individual pairwise comparisons by the Student-Newman Keuls test.

Figure 5. Hematopoietic specific ROCK1 deficiency attenuates skin inflammation with decreases in exhibition of NET-associated pro-inflammatory cytokines in UVB-irradiated BMT-ROCK1$^{+/-}$ mice. **A-I**. Summary analyses (**A**,**D**,**F**,**H**) and representative images (**B**,**C**,**E**,**G**,**I**) of skin sections of BMT-WT vs BMT-ROCK1$^{+/-}$ mice that were irradiated without (sham) or with UVB, and stained of neutrophil surface marker Ly6G by PE-conjugated rat anti-mouse **Ly6G** Ab, and FITC labeled Rat anti-mouse **IL-17A**, **TNFα**, **IFNγ**, or **IFNα**. DNA was stained by **DAPI** for panels **A-I**. Arrows indicate NETotic neutrophils in images of different panels. Scale bars, 100μm. In the panels A,C,E,G, P<0.01 by ANOVA; displayed are significance levels for individual pairwise comparisons by the Student-Newman Keuls test.

Figure 6. Genetic deficiency of ROCK1 decreases formation of NETs and attenuates their exhibition of pro-inflammatory cytokines in neutrophils from ROCK1 deficient mice. **A-I**.

Summary analyses (**A**,**C**,**E**,**G**) and representative images (**B**,**D**,**F**,**H**) of BM neutrophils from ROCK1$^{+/-}$ mice or their WT littermates were treated without or with 10 μM PAF (for IFNα induction in G-H, treatment with PAF and isolated NETs from neutrophils of MRL/lpr mice) for overnight, following by fixation and immunocytochemistry staining of neutrophils by PE-conjugated anti-mouse **Ly6G** Ab, FITC labeled anti-mouse **IL-17A**, **TNFα**, **IFNγ**, or **IFNα**. DNA was stained by **DAPI**. Scale bars, 50μm. Arrows indicate NETs with extracellular exhibition of different cytokines. All results are representative of 3 independent experiments. In the panels A,C,E,G, $P<0.01$ by ANOVA; displayed are significance levels for individual pairwise comparisons by the Student-Newman Keuls test.

Figure 1.

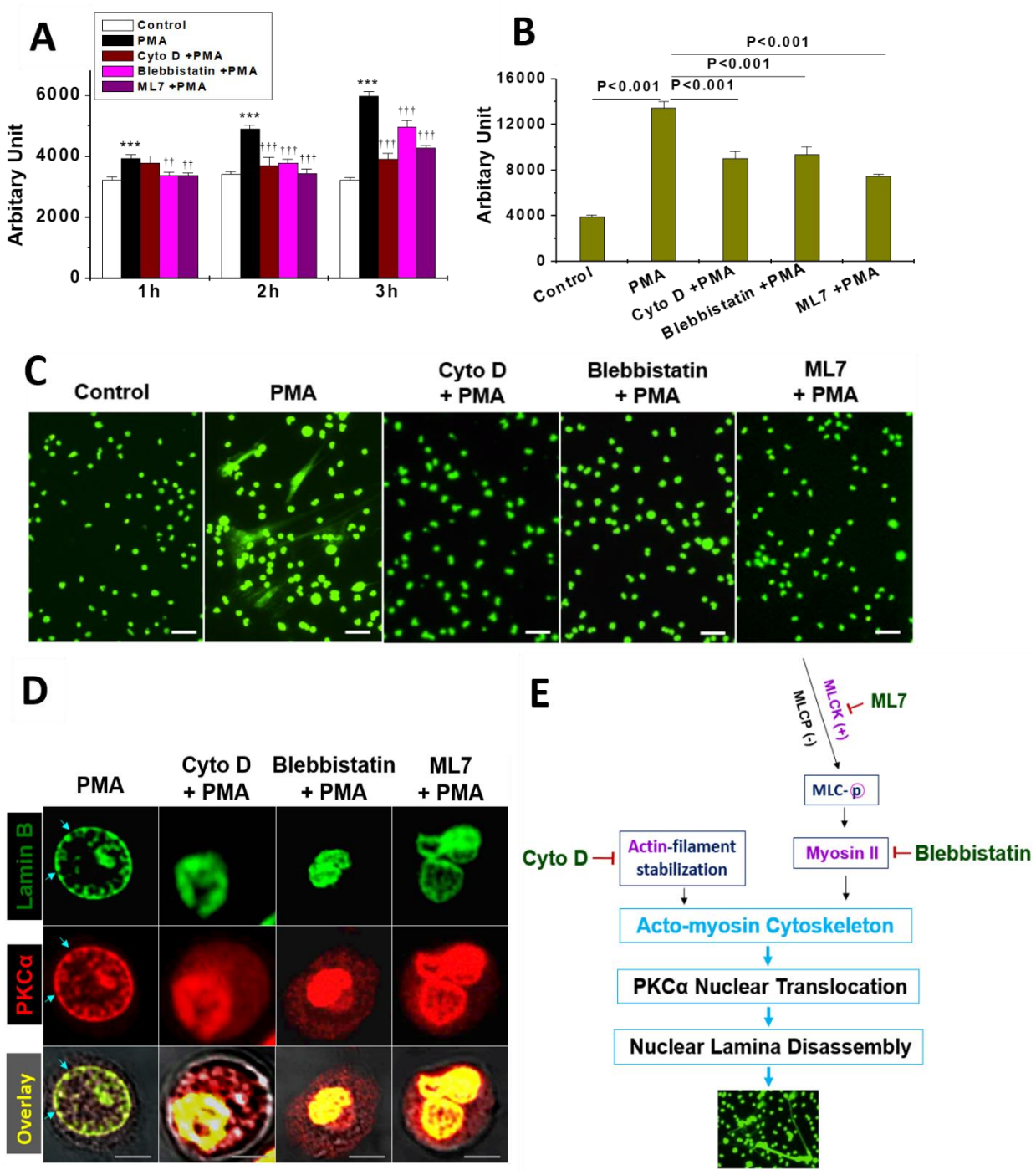
A
Control
PMA
Cyto D +PMA
Blebbistatin +PMA
ML7 +PMA
Arbitary Unit
6000
4000
2000
0
1h
2h
3h
B
P<0.001
P<0.001
P<0.001
P<0.001
16000
12000
8000
4000
0
Arbitary Unit
Control
PMA
Cyto D +PMA
Blebbistatin +PMA
ML7 +PMA
C
Control
PMA
Cyto D + PMA
Blebbistatin + PMA
ML7 + PMA
D
PMA
Cyto D + PMA
Blebbistatin + PMA
ML7 + PMA
Lamin B
PKCα
Overlay
E
MLCP (-)
MLCK (+)
ML7
MLC-ⓟ
Cyto D
Actin-filament stabilization
Myosin II
Blebbistatin
Acto-myosin Cytoskeleton
PKCα Nuclear Translocation
Nuclear Lamina Disassembly

Figure 2.

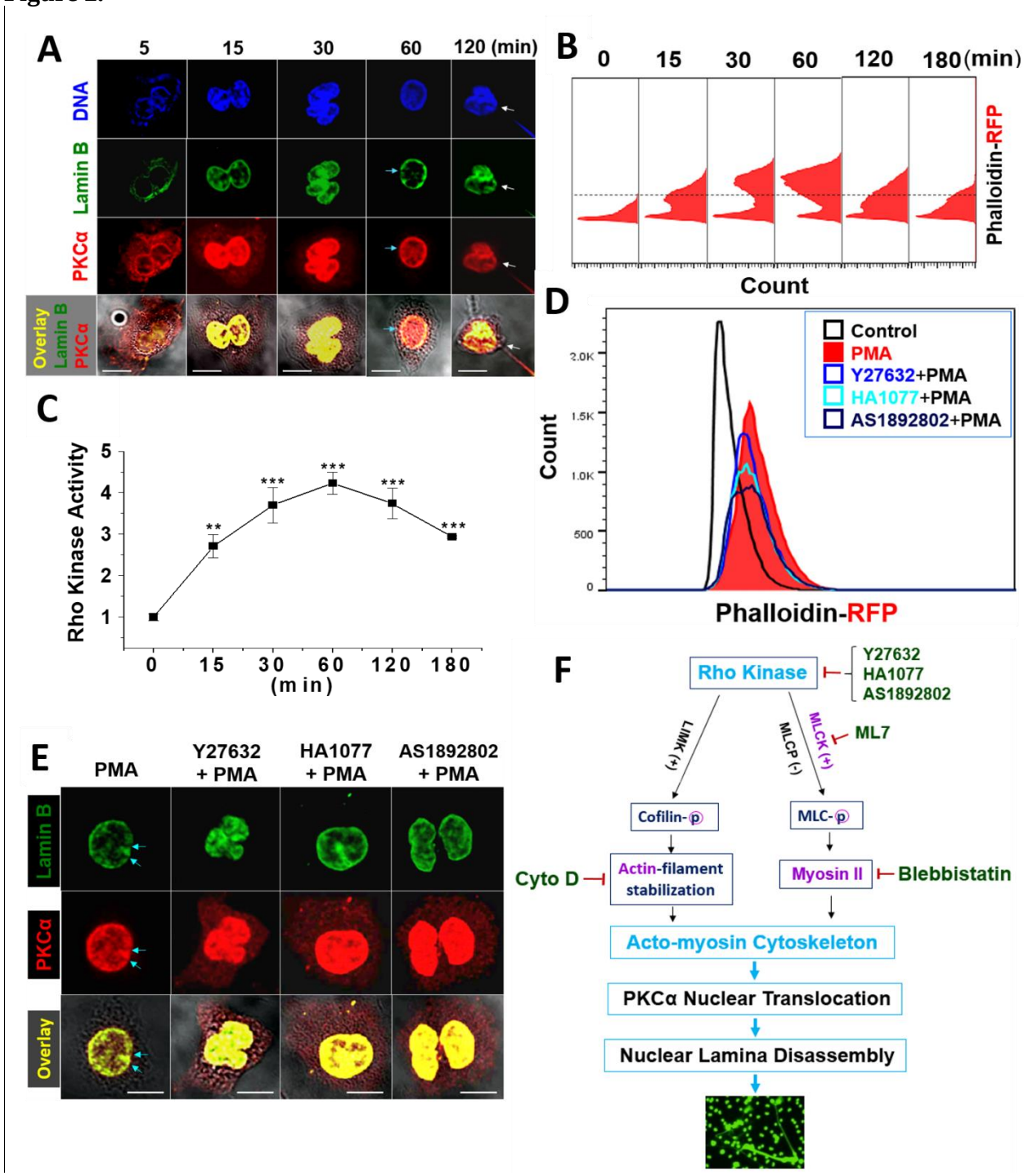
A
5
15
30
60
120 (min)
DNA
Lamin B
PKCα
Overlay
Lamin B
PKCα
B
0
15
30
60
120
180 (min)
Phalloidin-RFP
Count
C
Rho Kinase Activity
(min)
D
Control
PMA
Y27632+PMA
HA1077+PMA
AS1892802+PMA
Count
Phalloidin-RFP
E
PMA
Y27632 + PMA
HA1077 + PMA
AS1892802 + PMA
Lamin B
PKCα
Overlay
F
Rho Kinase
Y27632
HA1077
AS1892802
LIMK (+)
MLCP (-)
MLCK (+)
ML7
Cofilin-ⓟ
MLC-ⓟ
Cyto D
Actin-filament stabilization
Myosin II
Blebbistatin
Acto-myosin Cytoskeleton
PKCα Nuclear Translocation
Nuclear Lamina Disassembly

Figure 3.

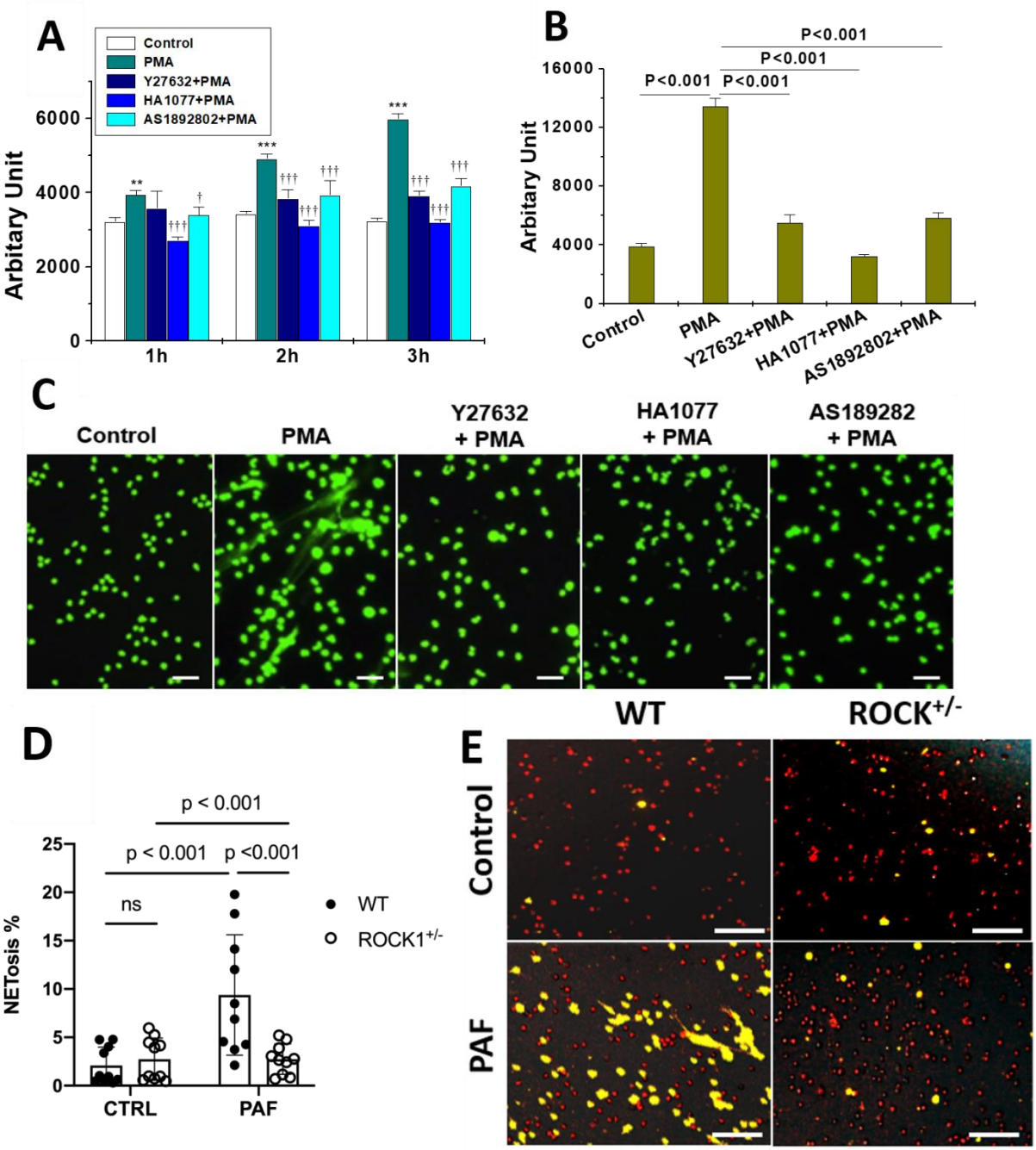
A
Control
PMA
Y27632+PMA
HA1077+PMA
AS1892802+PMA
Arbitary Unit
1h
2h
3h
B
P<0.001
P<0.001
P<0.001
P<0.001
Arbitary Unit
Control
PMA
Y27632+PMA
HA1077+PMA
AS1892802+PMA
C
Control
PMA
Y27632 + PMA
HA1077 + PMA
AS189282 + PMA
D
p < 0.001
p < 0.001
p <0.001
ns
NETosis %
WT
ROCK1+/-
CTRL
PAF
E
WT
ROCK+/-
Control
PAF

Figure 4.

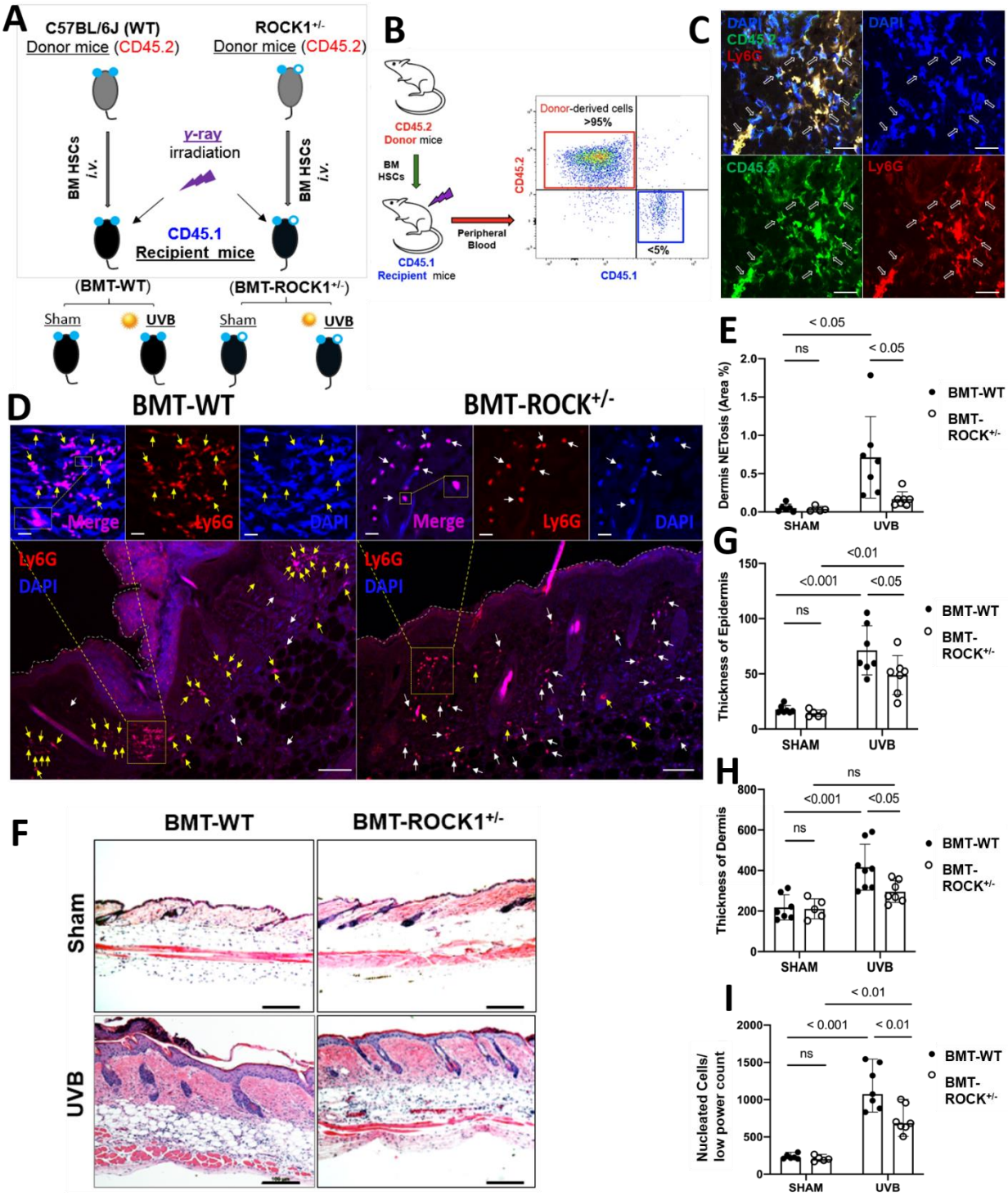
A
C57BL/6J (WT)
Donor mice (CD45.2)
ROCK1+/-
Donor mice (CD45.2)
BM HSCs i.v.
γ-ray irradiation
CD45.1
Recipient mice
(BMT-WT)
(BMT-ROCK1+/-)
Sham
UVB
B
CD45.2
Donor mice
BM HSCs
CD45.1
Recipient mice
Peripheral Blood
Donor-derived cells >95%
<5%
CD45.2
CD45.1
C
DAPI
CD45.2
Ly6G
D
BMT-WT
BMT-ROCK+/-
Merge
Ly6G
DAPI
E
Dermis NETosis (Area %)
SHAM
UVB
BMT-WT
BMT-ROCK+/-
G
Thickness of Epidermis
H
Thickness of Dermis
I
Nucleated Cells/ low power count
F
BMT-WT
BMT-ROCK1+/-
Sham
UVB

Figure 5.

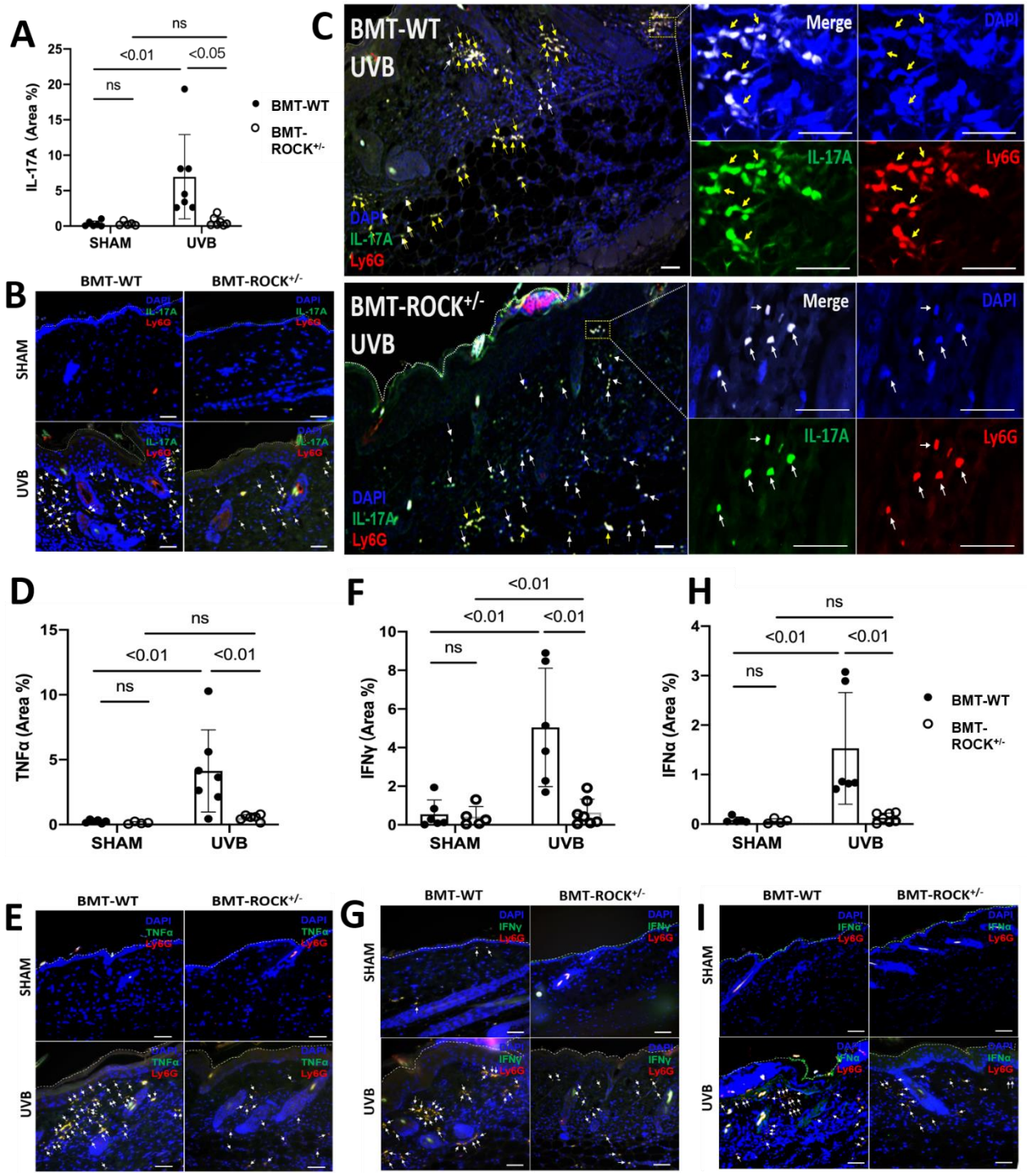
A
IL-17A (Area %)
ns
<0.01
<0.05
ns
SHAM
UVB
BMT-WT
BMT-ROCK+/-
B
BMT-WT
BMT-ROCK+/-
SHAM
UVB
DAPI
IL-17A
Ly6G
C
BMT-WT
UVB
Merge
DAPI
IL-17A
Ly6G
BMT-ROCK+/-
UVB
D
TNFα (Area %)
ns
<0.01
<0.01
ns
SHAM
UVB
F
IFNγ (Area %)
<0.01
<0.01
<0.01
ns
SHAM
UVB
H
IFNα (Area %)
ns
<0.01
<0.01
ns
SHAM
UVB
BMT-WT
BMT-ROCK+/-
E
BMT-WT
BMT-ROCK+/-
SHAM
UVB
DAPI
TNFα
Ly6G
G
BMT-WT
BMT-ROCK+/-
SHAM
UVB
DAPI
IFNγ
Ly6G
I
BMT-WT
BMT-ROCK+/-
SHAM
UVB
DAPI
IFNα
Ly6G

Figure 6.

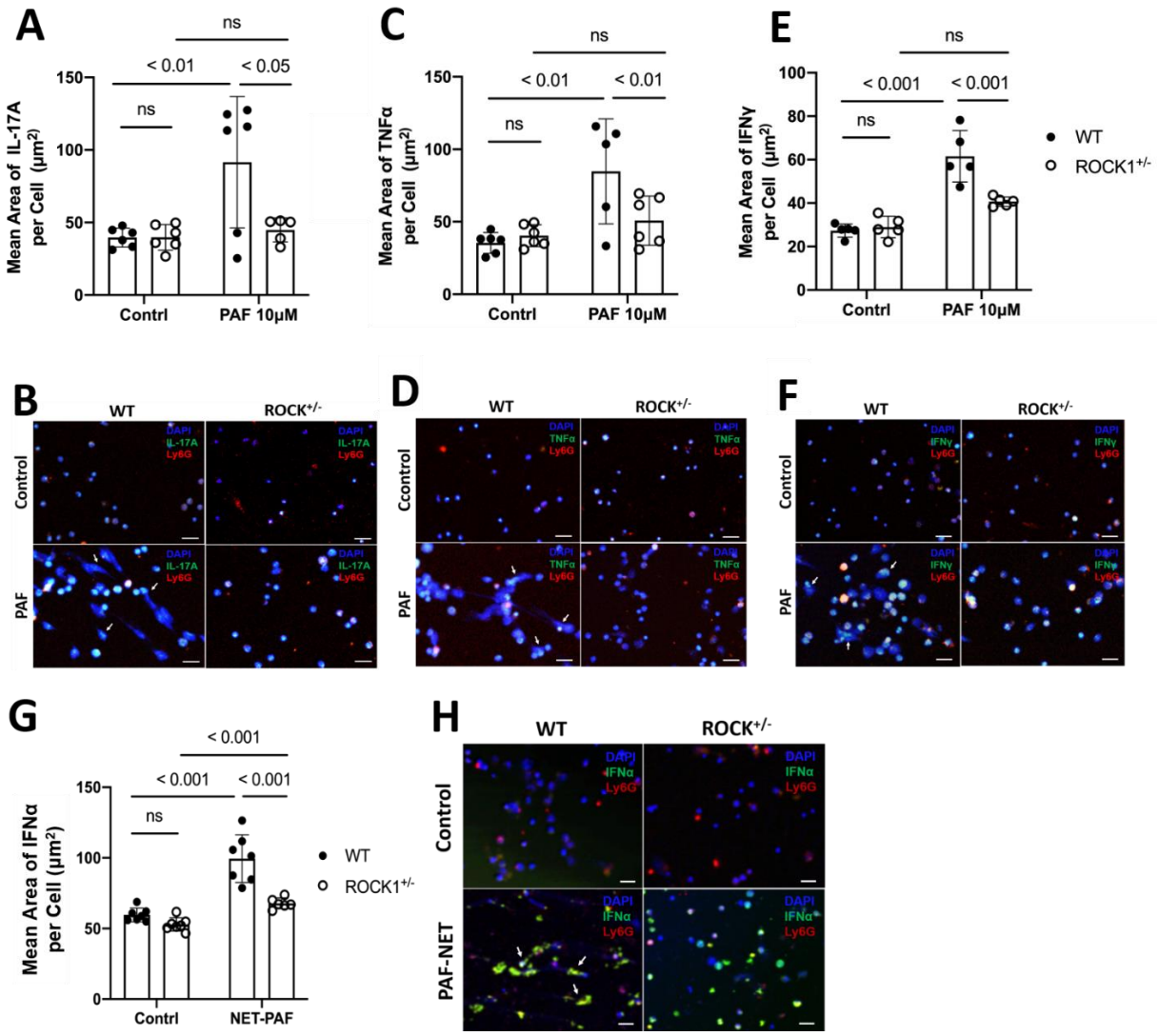
A
ns
< 0.01
< 0.05
ns
Mean Area of IL-17A per Cell (μm²)
Contrl
PAF 10μM
C
ns
< 0.01
< 0.01
ns
Mean Area of TNFα per Cell (μm²)
Contrl
PAF 10μM
E
ns
< 0.001
< 0.001
ns
Mean Area of IFNγ per Cell (μm²)
WT
ROCK1+/-
Contrl
PAF 10μM
B
WT
ROCK+/-
Control
PAF
DAPI
IL-17A
Ly6G
D
WT
ROCK+/-
Ccontrol
PAF
DAPI
TNFα
Ly6G
F
WT
ROCK+/-
Control
PAF
DAPI
IFNγ
Ly6G
G
< 0.001
< 0.001
< 0.001
ns
Mean Area of IFNα per Cell (μm²)
WT
ROCK1+/-
Contrl
NET-PAF
H
WT
ROCK+/-
Control
PAF-NET
DAPI
IFNα
Ly6G

Supplemental Materials

Deficiency of Rho Kinase 1 (ROCK1) attenuates neutrophil NETosis and ameliorates UVB-induced skin inflammation

Running title: ***Rho kinase and NETosis***

Supplemental Methods

Generation of hematopoietic deficient mice by bone marrow transplantation (BMT). To generate mice with hematopoietic specific ROCK1 deficiency, or their corresponding background control mice, BMT was conducted according to our established BMT techniques by following the approved animal protocol, as described (1) with modification. In brief, the BM hematopoietic stem cells (HSCs, >5x10^6 cells) were harvested from the femur and tibia of donor ROCK1$^{+/-}$ mice or their littermate WT (all 6-8-week-old, with CD45.2 congenic background). The donor HSCs (>5x10^6 cells) from either ROCK1$^{+/-}$ or WT mice were transplanted into sex-matched CD45.1 recipient mice (all 6-8-week-old) which were pre-irradiated sub-lethally with two equal doses of 550 cGy (*Total Body Irradiation* 1100 cGy) at intervals of 18 hours (2, 3) with a *Cs-137 Irradiator* (1). From one-week prior the BMT, mice were given medicated acidified water with antibiotics (sulfamethoxazole and trimethoprim) until 6 weeks post BMT. Mice were given soften food and kept in animal biosafety level 2 room immediately after irradiation and BMT for up to 6 weeks until UVB exposure. Peripheral blood chimerism was analyzed by flow cytometry analysis of reconstitution rate of CD45.2 cells in the

peripheral blood of CD45.1 recipient mice at 4 weeks post BMT as a functional assay of HSC fitness. Only successfully transplanted mice (over 95% reconstitution) were used in later animal experiments.

UVB Exposure. The dorsal skins of CD45.1 mice with hematopoietic specific ROCK1 deficiency (BMT-ROCK1$^{+/-}$), or their corresponding control mice (BMT-WT) were irradiated or not (sham groups) by UVB (150 mJ/cm^2/day) for 5 consecutive days under anesthetization by peritoneal injected Ketamine/Xylazine (4). Each group includes 6-8 mice with half-male and half-female studied. Animals were then sacrificed 24 hours after the last exposure. The whole dorsal skin samples, including epidermis, dermis, and subcutaneous fat were collected. Tissue sample sectioning was performed by the Penn Skin Biology and Diseases Resource-based Center. The skin sections from both UVB-irradiated and sham-irradiated mice were stained for hematoxylin and eosin (H&E). Infiltration of inflammatory cells was counted for the nucleated cells in the epidermis, dermis, or fat (5, 6).

Supplemental Figures

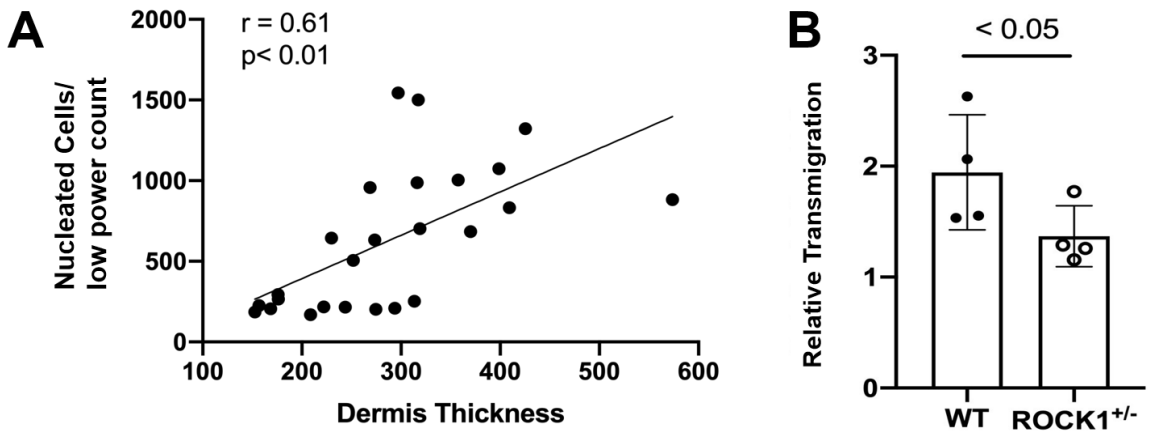

Supplementary Figure 1. A. Correlation analysis between infiltration of inflammatory (nucleated) cells and thickness of dermis. **B**. Relative migration analysis of BM neutrophils from WT vs ROCK1$^{+/-}$ mice was conducted with Boyden chamber (n=4 in each group). Panel A was conducted by Pearson correlation analysis. Panel B was analyzed by paired student's t-test.

References

1. Duran-Struuck R, and Dysko RC. Principles of bone marrow transplantation (BMT): providing optimal veterinary and husbandry care to irradiated mice in BMT studies. *J Am Assoc Lab Anim Sci.* 2009;48(1):11-22.
2. Down JD, Tarbell NJ, Thames HD, and Mauch PM. Syngeneic and allogeneic bone marrow engraftment after total body irradiation: dependence on dose, dose rate, and fractionation. *Blood.* 1991;77(3):661-9.
3. Marino R, Otsuru S, Hofmann TJ, Olson TS, Rasini V, Veronesi E, Boyd K, Gaber MW, Martinez C, Paolucci P, et al. Delayed marrow infusion in mice enhances hematopoietic and osteopoietic engraftment by facilitating transient expansion of the osteoblastic niche. *Biol Blood Marrow Transplant.* 2013;19(11):1566-73.
4. Li Y, Li M, Weigel B, Werth VP, Mall M, and Liu ML. Nuclear envelope rupture and NET formation is driven by PKCα-mediated lamin B disassembly. *EMBO reports.* 2020;21(e48779).
5. Menke J, Hsu MY, Byrne KT, Lucas JA, Rabacal WA, Croker BP, Zong XH, Stanley ER, and Kelley VR. Sunlight triggers cutaneous lupus through a CSF-1-dependent mechanism in MRL-Fas(lpr) mice. *J Immunol.* 2008;181(10):7367-79.
6. Sontheimer C, Liggitt D, and Elkon KB. Ultraviolet B Irradiation Causes Stimulator of Interferon Genes-Dependent Production of Protective Type I Interferon in Mouse Skin by Recruited Inflammatory Monocytes. *Arthritis Rheumatol.* 2017;6